SYNTHESIS OF ZINC FERRITE USING CERAMIC METHOD

Mery Cecilia Gómez Marroquín[1], José Carlos D'Abreu[2], Dirson Carlos Herrera, Jhon Cano Sovero, Gianmarco Roa Bernardillo, Jhon Condori Yalli

Catholic University of Rio de Janeiro - Puc-Rio
Materials Science and Metallurgy Department (DCMM)
Rua Marquês de São Vicente 225. Gávea - RJ. CEP 22453-900
Rio de Janeiro - Brazil

[1]e-mail:mgomezm@uni.edu.pe
[2]e-mail:dabreu@puc-rio.br

Abstract

Zinc ferrite is a compound commonly used in the electronic industries and also present in some kinds of dusts generated in steelmaking plants. The present work deals with the kinetics of the zinc ferrite synthesis, occurring through a solid-solid reaction in a selected range of temperatures, using as reactant an equimolar mixture of pure iron oxide- Fe_2O_3 and pure zinc oxide - ZnO. This equimolar mixture was thermally characterized using the DTA and TGA techniques. In sequence the zinc ferrite produced were examined using X-Ray Diffraction, Scanning and Transmission Electronic Microscopy. Finally the software Topas 2.1, Difrac Plus, using the Rietveld XRD method was applied to calculate the amount of zinc ferrite generated during the synthesis reaction. The main aiming of this project was analyze the zinc ferrite generated in laboratory in the conditions of the Electric Arc Furnace dusts formation, in the temperature range from 873 to 1273 K, aiming at future zinc recycling.

Keywords - Zinc ferrite; Kinetics; Characterization; Steel making dusts

1. Introduction

Zinc ferrite formation is of interest to both the electronics and the metallurgy industries. In the electronics industry, it has been found that both the magnetic and the electrical properties of ferrites can be substantially improved if some zinc oxide is presented. In the metallurgical industry, zinc ferrite is found in the calcine from the roasting of zinc ores and also in the Electric Arc Furnace-EAF dusts, which is generated when galvanized scrap proceeding to the automotive industry is melted in the Electric Arc Furnace-EAF. (Xia D. K. & Pickles C. A., 1997). EAF dusts contains about 30% zinc, of which 70% is in the form of zinc ferrite and the remaining 30% as zinc oxide. (Hsi-Kuei Chen et. al, 2001).

Zinc ferrite is also known as an advanced mixed-metal sorbent for high-temperature desulfurization of coal gas. This removes hydrogen sulfide from hot coal-derived gas streams and can operate at temperatures and pressures matching typical gasifier outlet conditions (Kim Wantae & Saito Fumio, 2000).

Three different methods were used to produce dense $ZnFe_2O_4$ ceramics with high electrical resistance – spray pyrolysis (SP), conventional sintering (CS) and spark plasma sintering (SPS). The phase purity was determined by X-ray diffraction and the morphology/particle size investigated by scanning electron microscopy. It was found that SP is the most appropriate method to produce a dense ZnFe2O4 ceramics with high electrical resistivity. By using the SP method, about 500 nm thick $ZnFe_2O_4$ films were obtained possessing a resistivity with 7 orders of magnitude higher than resistivity of $ZnFe_2O_4$ pellet sintered by SPS. Both samples obtained by SP and SPS show density close to the theoretical value. The sample obtained by CS shows a low resistivity and relatively high porosity (Sutka A. *et al*, 2013). Another hand a spray pyrolysis of a water solution of iron, manganese and iron nitrates is applied to prepare $Zn_{0.5}Mn_{0.5}Fe_2O_4$ single-phase ferrite with a spinel-type structure. The samples are characterized by means of differential scanning calorimetry, scanning and transmission electron microscopy, X-ray diffraction, infrared and 57Fe Mossbauer spectroscopy. The mass magnetization € s and the magnetic susceptibility 1/c of the ferrites are measured as a function of temperature over the range of 78e728 K. The obtained sample contains nanoparticles with an average diameter d ~7 nm possessing $MnxZnyFe_3$-(x+y)O_4 spinel-type structure with a uniform distribution of manganese and zinc atoms over the ferrite lattice. The Curie temperature was determined to be 375 ÷ 380 K (Kotsikau, *et al*, 2015).

Zinc ferrite is a normal spinel, whose tetrahedral A-site and octahedral B-site are partially occupied by Zn^{+2} and Fe^{+3} cations, respectively. The partial replacement of Zn^{+2} and Fe^{+3} by others metals in different oxidation states yields to mixed ferrites with different magnetic properties (López-Delgado A. *et al.*, 1998).

The conventional synthesis of spinel ferrites starts from elemental oxide powders mixtures, which are milled, formed and finally sintered at temperatures above 1300ºC (Botta P. M. et al , 2005).

Pure and lanthanum doped zinc ferrite nanoparticles were synthesized by a combustion method using glycine as fuel. The combustion method significantly produces large amount of products within a short time. Therefore, this method is potentially suitable for manufacturing industries for preparing the magnetic nanoparticles (Tholkappiyan, R., & Vishista, K., 2014).

Single-phase nanocrystalline zinc ferrite (ZnFe2O4) spinel powders have been successfully synthesized by an easy homogeneous precipitation method in short precipitation time at low calcination temperature (250 °C). The spinel $ZnFe_2O_4$ powders consist of spherical nanoparticles with an average size of 5.270.61 nm. The antifungal activity of the nanocrystalline zinc ferrite powders was tested against pathogenic Candida albicans using the disc-diffusion susceptibility method. The nanocrystalline zinc ferrite powders exhibit strong antifungal activity against pathogenic *C. Albicans* (Sharma, R. K., & Ghose, R., 2015).

Mechanochemical reaction of ZnO and α-Fe_2O_3 processing is a novel and cheap method for the production of nanoparticles of zinc ferrite. However, few report has focused on the mechanochemical preparation of $ZnFe_2O_4$ nanocrystallites (Yang Huaming et al, 2004). To the best of our knowledge, so far, the phase transformation kinetics of ball-milled ferrites have not yet been studied in detail by X-ray powder structure refinement method (Bid S. & Pradhan S. K., 2002).

The mechanism of the zinc ferrite formation is explained as three-step process: (ii) ZnO migrates to the α-Fe_2O_3 grains, due to its higher mobility, (ii) Zn in the tetrahedral site of ZnO redistributes itself into the tetrahedral site of spinel in order to form the ferrite at the surface of hematite grains and (iii) the zinc ferrite grain containnig Zn diffuses through the ferrite layers towards the hematite lattice for further growth of the ferrite (Bera S. et al, 2001), at the time the nucleation of zinc ferrite was retarded in reaction mixtures of ZnO e Fe_2O_3 with an excess of Fe_2O_3. The presence of ZnO, in ratios higher than equimolar, accelerated the reaction. Reaction data were analyzed using kinetic equations corresponding to models of (a) diffusion, (b) nucleation and (c) phase boundary reaction. After an initial period at low temperature, during which the interface reaction rate and diffusion through the layer product contributed comparably to the reaction rate, the reaction in equimolar mixtures was approximated by the diffusion equations. This author, using the Ginstling-Brounshtein's equation, found activation energy of 117 kJ/mol for temperatures between 873-1073K (Halikia I. & Milona E., 1994).

Zinc ferrite formation is relativity simple solid-state reaction and is often selected as a model system for homogeneous rate process. The initial surface chemical reaction involved in zinc ferrite formation is very rapid at any given temperature, and the reactants quickly become covered with zinc ferrite. Then, the reaction rate becomes decelerated. The kinetics of zinc ferrite formation was studied in the temperature range of 873-1073 K and results were best described by Jander's diffusion model with energy of activation of 168 kJ/mol (Xia D. K. & Pickles C. A., 1997).

-Shimizu, Akira 1998, reported that the Jander model represented the most suitable kinetics solid-state reactions model of the zinc ferrite formation:

$$[\,1-(\,1-\alpha\,)^{\,1/3}\,]^{\,2} = k\,t$$

Ultrasonic treatment significantly affects the kinetics and mechanism of the solid-phase synthesis of the zinc ferrite, which is likely due to the formation of a more extended reaction zone at the initial stage of the reaction. The apparent activation energy obtained were (a) 158 ± 7 kJ/mol for solid-phase reaction and (b) 138 ± 11 kJ/mol on the common thermal treatment (Baranchikov A. E. et al., 2004) and during the thermal treatment, the formation of $ZnFe_2O_4$ was significantly increased by the previous mechanical treatment, reaching high conversions at temperatures lower than those used in conventional synthesis methods. For the active powder mixtures, the formation of $ZnFe_2O_4$ is governed by the nucleation and growth of the product phase, unlike the diffusional control reported for the conventional system. The calculated activation energy value obtained for temperatures between 963 -1033K was 300 kJ/mol (Botta P.M. et al., 2006).

The main aiming of this project was analyze the zinc ferrite generated in laboratory in the conditions of the Electric Arc Furnace dusts formation, in the temperature range from 873 to 1273 K, aiming at future zinc recycling.

2. Experimental procedures

2.1 Raw Materials

The raw materials used in the study of zinc ferrite formation were zinc oxide (ZnO) and iron oxide III (Fe_2O_3) with 99.999 % purity.

2.2 Heat Treatment

Samples of equimolar mixture were milled in mortar during 35-60 min to ensure uniform mixtures. Specimens weighing 5-7 g were pressed in a 254 mm diameter cylindrical shell die under a pressure of 400-500 MPa. The pressed briquettes were heated in isothermals conditions in an electric horizontal furnace of 1373 K of maximum temperature.

The temperatures of reactions were of 873, 923, 973, 1003, 1023, 1073 and 1273 K with time of reaction of 0.5, 1, 2, 3, and 4 hours respectively.

2.3 Characterization by DTA-TGA

In order to obtain thermic information about of the zinc ferrite formation; raw materials (pures oxides), stoichiometric mixtures (equimolar ratio) and non-stoichiometric mixtures was used.

These experiments were based mainly in a previous pre-treatment of iron oxide III, Fe_2O_3, zinc oxide, ZnO and mixtures of both oxides with following Fe_2O_3:ZnO molar ratios: 2:1 (79.68% Fe_2O_3 and 20.32% ZnO) 1:1 (66.67% Fe_2O_3 and 33.34% ZnO) 1:2 (49.49% Fe_2O_3 and 50.01% ZnO) and 1:4 (32.89 %Fe_2O_3 and 67.11% ZnO) respectively.

The following equipments were utilized by thermal characterization: Differential Thermal Analyzer, DTA (DTA-50 Shimadzu) and Thermogravimetric Analyzer, TGA (TGA-51 Shimadzu).

Each specimen of pure oxides and different mixtures were thermically characterized using a rate flow of nitrogen of 70 mL/min and a heat rate 20ºC/min. for both DTA and TGA equipments.

2.3 Structural Characterization by XRD

Solid samples heated under isothermal conditions were ground by a pestle and a mortar to fine powder for the XRD analysis.

X-Rays diffractometer model SIEMENS D5000, Kristalloflex utilizing a Copper anode K-α radiation (Cu K-α of λ=1.5406 Å), with an acceleration voltage of 40 kV and a current of 30 mA was used. The diffraction angle (2θ) was of de 5-80 deg was scanned and the rate was of 8 deg/min.

The synthesized products were then analyzed by XRD using the software Difracc Plus Topas 2.1 version of Bruker AXS (Rietveld's method), in order to determine the amounts of unreacted ZnO and Fe_2O_3 and the content of zinc ferrite formed ($ZnFe_2O_4$) after of heat treatment. This software is specially designed to refine simultaneously both structural and micro structural parameters through a least-squares method. The peak shape was assumed to be a pseudo-Voigt (pV) function with asymmetry. The background if each pattern was fitted by a polynomial function of degree three. In the present study, refinements were conducted without refining the isotropic atomic thermal parameters.

2.4 Microscopic Characterization

Scanning Electron Microscopy (SEM) and Transmission Electron Microscopy (TEM) were used to observe the morphology and particle size of zinc ferrite.

The appearance of the grains containing zinc ferrite, zinc oxide and iron oxide were observed with an SEM (DSM 960 model with 80 mA of current intensity and 20 kV of voltage) and TEM (JEOL 2010 model with 109 mA of current intensity and 200 kV of voltage) with probe size of 20 nm.

3. Results and discussion

3.1 DTA Characterization

In Fig. 1-a, are shown the DTA characterizations of mixtures of iron III oxide and zinc oxide with following Fe_2O_3:ZnO molar ratios: 2:1 (M2:1), 1:1 (M1:1- equimolar mixture), 1:2 (M1:2) and 1:4 (M1:4).

In Fig. 1-b, was shown the DTA curve of equimolar mixture, where one endothermic peak are noted at 653-1033 K (endothermic peak temperature 1033 K) and one exothermic peak at 1283-1517 K (exothermic peak temperature 1388 K) temperature range, respectively.

The clear endothermic peak appearing at 1033 K corresponds to the formation of $ZnFe_2O_4$ by heating the raw materials. In addition, the exothermic peak at 1388 K can be attributed to the recrystallization of $ZnFe_2O_4$ and rearrangement in its lattice (spinel formation).

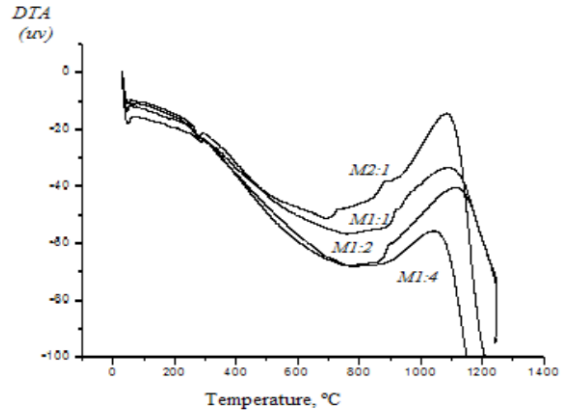

(a)

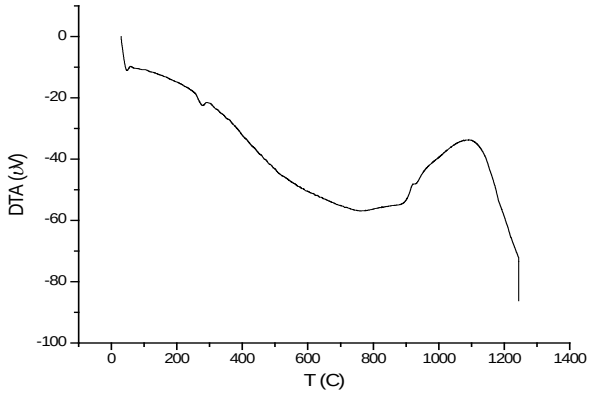

(b)

Figure 1. Differential Thermal Analyzer, DTA of mixtures with different molar ratios: Fe_2O_3/ZnO: 2/1, 1/1, 1/2 e 1/4 (a). DTA of equimolar mixture, Fe_2O_3/ZnO:1/1 (b).

3.2 TGA Characterization

In Figure 2-a, are shown the TGA characterizations of iron III (Fe_2O_3) oxide and zinc oxide (ZnO) and mixtures of the both oxides with following Fe_2O_3:ZnO molar ratios: M2:1 M1:1 (equimolar mixture), M1:2 and M1:4 where is observed that the mass loss of mixtures and oxides were minimum. Specifically in Figure 2-b the mass loss for the equimolar mixture corresponds at 0.009%.

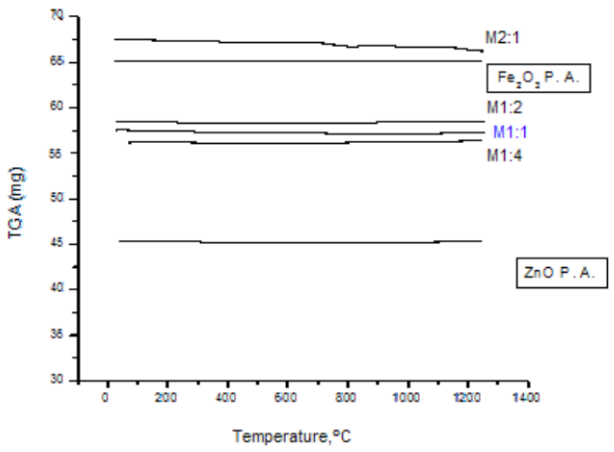

(a)

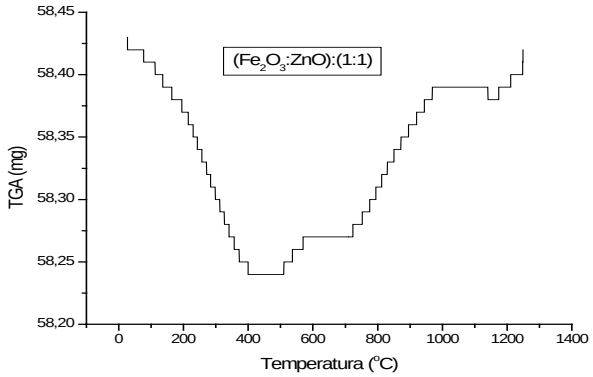

(b)

Figure 2. Thermogravimetric Analyzer, TGA of pure oxides Fe_2O_3 e ZnO, and mixtures with different molar ratios: Fe_2O_3/ZnO : 2/1, 1/1, 1/2 e 1/4 (a). TGA of equimolar mixture, Fe_2O_3/ZnO:1/1 (b).

3.3. XRD Characterization

The formation of zinc ferrite phase is initiated by the solid-state diffusion process, ZnO + Fe_2O_3 = $ZnFe_2O_4$, which is detected by XRD studies.

Figure 3 shows XRD powder patterns of equimolar zinc ferrite produced after heating at 923 K during 10 minutes (a) and 1273 K during 4 hours (b).

In both Figure 3-a and Figure 3-b the $ZnFe_2O_4$ phase growth at the expense of ZnO and Fe_2O_3 phases is shown by the decrease in the intensity of diffraction lines related to ZnO and Fe_2O_3 phases and the results of refining of XRD patterns diffraction.

The results of refined XRD patterns by Rietveld's method were: 0.67% $ZnFe_2O_4$, 68.34% Fe_2O_3 and 30.99% ZnO (Figure 3-a) and 97.60% $ZnFe_2O_4$, 2.00% Fe_2O_3 and 0.40% ZnO (Figure 3-b) respectively.

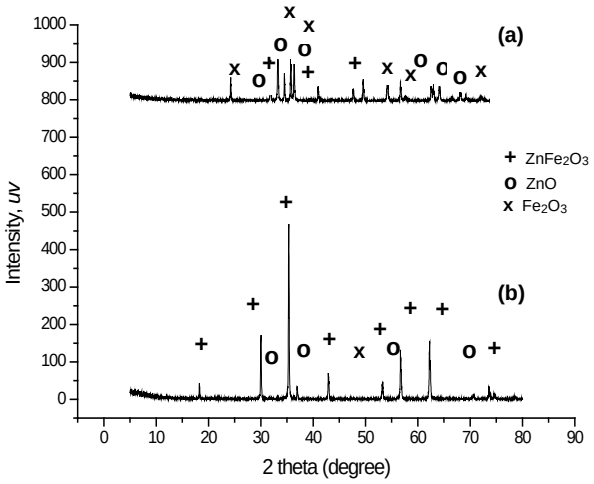

Figure 3. XRD patterns of equimolar zinc ferrite produced after heating at: 923 K during 10 minutes (a), and 1273 K during 4 hours (b).

3.4. Microscopic Characterization

In Figure 4 a SEM image is presented showing the predominant presence of zinc ferrite agglomerated with same porous in the shape of clusters.
In Figure 5 is a TEM image presenting small zinc ferrite particles having sizes of about 100 nm.

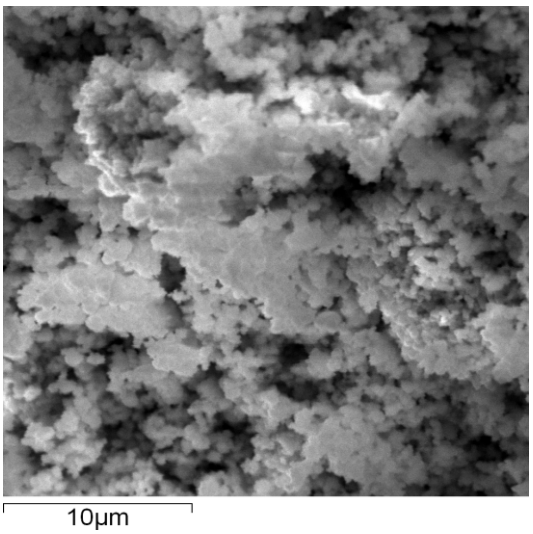

Figure 4. SEM of typical structures produced on equimolar zinc ferrite

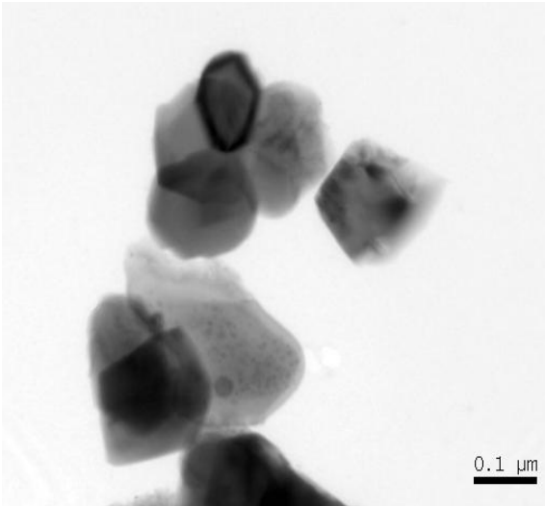

Figure 5. TEM of typical structures produced on equimolar zinc ferrite

5. Discussion

These experiments were based mainly in a previous pre-treatment of iron oxide III, Fe_2O_3, zinc oxide, ZnO and mixtures of both oxides with following Fe_2O_3:ZnO molar ratios: 2:1 (79.68% Fe_2O_3 and 20.32% ZnO) 1:1 (66.67% Fe_2O_3 and 33.34% ZnO) 1:2 (49.49% Fe_2O_3 and 50.01% ZnO) and 1:4 (32.89 %Fe_2O_3 and 67.11% ZnO) respectively.

According to the X-Ray diffraction analysis (Rietveld's method) the zinc ferrite formation starts to takes place before ten minutes of heating at 650ºC (923 K). Confirming that, the range determined by the DTA analysis for the process, using an equimolar mixture, stoichiometric, spans from 367.15 to 976.55ºC (640 to 1250 K). Further, the DTA curve exhibits at 760ºC (1033 K) an inflection point signal of an endothermic peak appeared at this temperature corresponding to the zinc ferrite nucleation. This result partially agrees with the 923-1053 K temperature range considered by Kolta G.A. et al. (1980).

The DTA curve shows a broad endothermic peak starting at 643 K and ending at 1253 K approximately. This broadness predicts the temperature range where the nucleation of the first zinc ferrite grain takes place. This technique was also used too to confirm the formation of 0.67% $ZnFe_2O_4$ determined by X-rays diffraction, which took place during the first ten minutes, at a temperature of 923 K.

The results of refined XRD patterns by Rietveld's method were: 0.67% $ZnFe_2O_4$, 68.34% Fe_2O_3 and 30.99% ZnO (Figure 3-a) and 97.60% $ZnFe_2O_4$, 2.00% Fe_2O_3 and 0.40% ZnO (Figure 3-b) respectively, permitted to emphasize a remarked relation between a reaction time and temperature heating in the reaction of both oxides in order to synthesize the zinc ferrite using the ceramic method.

5. Conclusions

-These experiments were based mainly in a previous pre-treatment of iron oxide III, Fe_2O_3, zinc oxide, ZnO and mixtures of both oxides with following Fe_2O_3:ZnO molar ratios: 2:1 (79.68% Fe_2O_3 and 20.32% ZnO) 1:1 (66.67% Fe_2O_3 and 33.34% ZnO) 1:2 (49.49% Fe_2O_3 and 50.01% ZnO) and 1:4 (32.89 %Fe_2O_3 and 67.11% ZnO) respectively.

-The previous experiences permitted to choose the equimolar mixture because its weight loss in TGA was low significant (0.009%).

-The DTA curve shows a broad endothermic peak starting at 643 K and ending at 1253 K approximately. This broadness predicts the temperature range where the nucleation of the first zinc ferrite grain takes place. This technique was also used too to confirm the formation of 0.67% $ZnFe_2O_4$ determined by X-rays diffraction, which took place during the first ten minutes, at a temperature of 923 K.

- Refined XRD patterns by Rietveld's method were: 0.67% $ZnFe_2O_4$, 68.34% Fe_2O_3 and 30.99% ZnO and 97.60% $ZnFe_2O_4$, 2.00% Fe_2O_3 and 0.40% ZnO respectively, permitted to emphasize a remarked relation between a reaction time and temperature heating in the reaction of both oxides in order to synthesize the zinc ferrite using the ceramic method.

-SEM image is presented showing the predominant presence of zinc ferrite agglomerated with same porous in the shape of clusters.

-TEM image presenting small zinc ferrite particles having sizes of about 100 nm.

6. Acknowledgments

To the support granted by governmental financing agency, CAPES and CNPq.

7. References

Baranchikov A. E., Ivanov V. K., Oleynikov N.N.,Ketsko V.A. & Tret'yakov Y. D., 2004. Zinc ferrite synthesis in an ultrasonic field. Russian Journal of Inorganic Chemistry 49,Vol.11, pp. 1646-1650.

Bera S., Prince A. A. M,. Velmurugan S., Raghavan P. S., Gopalan R., Panneerselvam G. & Narasimhan S. V., 2001. Formation of the zinc ferrite by solid-state reaction and its characterization by XRD and XPS. Journal of Materials Science 36, pp. 5379-5384.

Beretka J. & Ridge M.J., 1967. Formation of zinc ferrite at low temperatures. Nature Vol. 26, November 4, pp. 473-474.

Bid S. & Pradhan S. K., 2003. Preparation of zinc ferrite by high-energy ball-milling and microstructure characterization by Rietveld's analysis. Materials Chemistry and Physics No.82, pp. 27-37.

Botta P. M., Aglietti E. F. & Porto López J. M., 2006. Kinetic study of $ZnFe_2O_4$ formation from mechanochemically activated Zn-Fe_2O_3 mixtures. Materials Research Bulletin 41, pp.714-723.

Chen Hsi-Kuei & Yang Ching-Yi, 2001. A study on the preparation of zinc ferrite. Scandinavian Journal of Metallurgy, No.30, pp. 238-241.

Donald J. R. & Pickles C.A., 1996. Reduction of electric arc furnace dust with solid iron powder. Canadian Metallurgical Quartely. Vol.35, No. 3 pp. 255-267.

Dunkan J. F. & Steward D.J., 1967. Kinetics and mechanisms of formation of zinc ferrite. Transactions of the Faraday Society 63(532P) pp. 1031-1041.

Feltz E., & Martin A., 1987. Solid-state reactivity and mechanisms in oxide systems II. Inhibition of zinc ferrite formation in zinc oxide-α-iron (III) oxide mixtures with a large excess of α-iron (III) oxide. Reactivity of Solids. Vol.2, Issue 4, pp. 307-313.

Hagni A. M., Hangi R. D., & Demars C., 1991. Mineralogical Characteristics of Electric Arc Furnace Dos, JOM, "O Jornal dos Minerais, Metais e Sociedade de Materiais", pp. 28-30.

Halikia I. & Milona E., 1994. Kinetic study of the solid-state reaction between alpha-Fe_2O_3 and ZnO for zinc Ferrite formation. Canadian Metallurgical Quarterly 33 (2): April-June 1994. pp. 99-109.

Chen Hsi-Kuei, 2001. Kinetics study on the carbothermic reduction of zinc oxide. Scandinavian Journal of Metallurgy. Vol. 30 pp. 292-296.

Kotsikau, D., Ivanovskaya, M., Pankov, V., & Fedotova, Y. (2015). Structure and magnetic properties of manganese–zinc-ferrites prepared by spray pyrolysis method. Solid State Sciences, 39, 69-73.

Gómez Marroquín M. C., 2004. "Contribution to the study of formation and reduction of zinc ferrite". Thesis for to obtain the Master Degree presented to the Metallurgy and Materials Science Department of "Pontifícia Universidade Católica do Rio de Janeiro"- Brasil.

Gómez Marroquín M. C., D'Abreu J. C. & Kohler M. H., 2004. "Contribution to the kinetics study of zinc ferrite formation contained in EAF dusts". Work presented to the Self-Reduction and Cold Agglomeration Seminar, to the 59 th Annual Congress of ABM-International, São Paulo- Brasil, from 19 th to 22 th of July, 2004.

Gómez Marroquín M. C. & D'Abreu, 2005 "Thermodynamics study of the zinc ferrite reduction"; Work presented to the Self-Reduction and Cold Agglomeration Seminar, to the 60 th Annual Congress of ABM-International, Belo Horizonte-Minas Gerais-Brasil, from 25th to 28th July, 2005.

Gómez Marroquín M. C., D'Abreu J. C. &. Kohler M. H., 2006. "Kinetics study of zinc ferrite formation". Work presented to the raw materials for iron making area: coal, iron ore, fluxes and additives of XXXVI Iron making and Raw Materials Seminar - ABM, Ouro Preto - Minas Gerais – Brasil, from 12 th to 15 th of September, 2006.

Guaita F. J., Beltran H., Cordoncillo E., Carda J. B., & Escribano P., 1998. Influence of the precursors on the formation and the properties of $ZnFe_2O_4$. Journal of the European Ceramic Society 19, pp. 363-372.

Kim Wantae & Saito Fumio, 2001. Mechanochemical synthesis of zinc ferrite from zinc oxide and α-Fe_2O_3. Powder Technology, No.114. p.12-16.

Kolta G. A., El-Tawil S. Z., Ibrahim A. A. & Felix N. S.,1980. Kinetics and mechanism of zinc ferrite formation. Thermochimica Acta, 36, pp. 359-366.

Krishnamurthy K. R., Gopalakrishnan J., Aravamudan G. & Sastri M.V.C., 1974. Studies on the formation of zinc ferrite. Journal of Inorganic and Nuclear Chemistry Volume, 36, Issue 3, pp. 569-573.

Lee Jyh-Jen, Lin Chun-I, and Chen Hsi-Kuei, 2001. Carbothermal reduction of zinc ferrite. Metallurgical and Materials Transactions B. Volume 32B, pp.1033-1040.

Shimizu Akira, 1998. Suitable of the kinetics model for estimation of powder reaction rate. Powder Technology Vol. 100, pp. 24-31.

Lopez Delgado A. Martin de Vidales J. L., Vila E. López F.A., 1998. Synthesis of mixed ferrite with spinel-type structure from a stainless steelmaking solid waste. Journal of Alloys and Compounds, No. 281 pp. 312-317.

Sharma, R. K., & Ghose, R. (2015). Synthesis and characterization of nanocrystalline zinc ferrite spinel powders by homogeneous precipitation method. Ceramics International, 41(10), 14684-14691

Sutka, A., Stingaciu, M., Jakovlevs, D., & Mezinskis, G. (2014). Comparison of different methods to produce dense zinc ferrite ceramics with high electrical resistance. Ceramics International, 40(1), 2519-2522.

Tholkappiyan, R., & Vishista, K. (2014). Influence of lanthanum on the optomagnetic properties of zinc ferrite prepared by combustion method. Physica B: Condensed Matter, 448, 177-183.

Tong, Fui Lee, 2001. Reduction mechanisms and behavior of zinc ferrite-Part 1: pure Zn Fe_2O_4. Trans. Instn Min. Metall. (Sect. C: Mineral Processes. Extractive Metallurgy), 110, January-April 2001.

Tsuchiya Teizo, Miyake Yoshikasu, Shigehisa Takanori, Tomita Ayako & Watanabe Masahiko, 2005. Journal of Chemical Engineering of Japan. Vol. 38, No. 9 pp.727-733.

Valenzuela M. A. Bosch P., Jimenez -Becerrill J. & Quiroz O., I. Páez A., 2002. Preparation, characterization and Figurecatalytic activity of ZnO, Fe_2O_3 and $ZnFe_2O_4$. Journal of Figurechemistry and Figurebiology A: Chemistry 148, pp.177-182.

Xia D. K. & Pickles C. A., 1997. Kinetics of zinc ferrite formation in the rate deceleration period. Metallurgical and Materials Transactions B. Volume 28 B, August 1997 pp. 671-677.

Yang Huaming, Zhang Xiangchao, Huang Chen, Yang Wuguo & Qiu Guanzhou, 2004. Synthesis of $ZnFe_2O_4$ nanocrystallites by mechanochemical reaction. Journal of Physical and Chemistry of Solids. Vol.65, pp.1329-1332.